ISSN: 0975-5772

Uday Chandra Kumar et al / Journal of Pharmaceutical Science and Technology Vol. 3 (1), 2011,536-542

3-D QSAR CoMSIA Models of Arylamides for Prediction of Enoyl Acyl Carrier Protein Reductase Inhibitory Activity

Uday Chandra Kumar and Mahmood Shaik
Bioinformatics Division, Environmental Microbiology Lab, Department of Botany, Osmania University, Hyderabad 500 007, A.P., India

Abstract:
Enoyl acyl carrier protein reductase is one of the key enzymes involved in the type II fatty acid biosynthesis pathway of M. tuberculosis. COMSIA analysis was performed using the molecular modeling package SYBYL 6.7.1 on silicon graphics work-station. A dataset of 28 Arylamide analogues reported to have Enoyl acyl carrier protein reductase inhibitory activities were used for the following QSAR studies. The CoMSIA models yielded a good cross-validated correlation coefficient with LOO of 0.744 and with leave-many-out (q2 with 10 groups) was 0.743, thus the predictions obtained with these models were reliable. The conventional correlation coefficient, r2 between the actual and estimated activities of the molecules was observed as 0.987, using this model. The test set compatibility was substantiated by the r2 pred value of 0.900. From QSAR studies the results have shown that Arylamide derivatives were proved to be highly potent inhibitors against Mycobacterium tuberculosis enoyl acyl carrier protein reductase.

Keywords: Comparative Molecular Similarity Indices Analysis; 3D-QSAR; Arylamide; Enoyl acyl carrier protein reductase; Mycobacterium tuberculosis

1. INTRODUCTION

People more than 1.6 million per year were reported to have died due to Tuberculosis (TB) and about 8.8 million new cases are reported every year. Such a big number of people affected by TB indicate this disease as the most dangerous and fatal infectious disease. TB is overpowered by only AIDS among the infectious diseases. According to the data collected by World Health Organization, people suffering from multi-drug-resistance and extensively drug-resistant TB are increasing with at least a half million new cases being reported every year. Therefore, it has become necessary for the researchers to synthesize novel TB drugs (1).

The chronic infectious disease tuberculosis is caused by *Mycobacterium* species of the 'tuberculosis complex', which include *Mycobacterium bovis*, *Mycobacterium africanum*, and mainly *Mycobacterium tuberculosis*. Compared to other infectious diseases, TB has become more fatal to many adults. Isoniazid is known to be effective drug against TB when used in combination with other anti-TB drugs. Serious conditions like multi-drug resistant TB (MDR-TB) and extensively drug resistant TB (XDR-TB) are unsolved public health problems now (2–7).

Isoniazid (isonicotinic acid hydrazide, INH) which was discovered in 1952 is accepted now as the most important drug for the treatment of TB. It is a pro-drug which is processed later during metabolic oxidation by the M. tuberculosis enzyme, catalase-peroxidase katG (5, 8, and 9).

2. MECHANISM

The INH-NAD(P) adducts were known to play role in preventing the action of the two enzymes called NAD-dependent enoyl-acyl carrier protein reductase (enoyl-ACP reductase, InhA) and NAD(P)-dependent beta-keto-ACP reductase (Mycolic acid biosynthesis A, MabA) which are involved in the fatty acid biosynthetic pathway of M. tuberculosis (10–13, 14).

Mechanism of action of INH and ETH.

The pro-drugs INH and ETH are triggered by the Catalase-Peroxidase KatG or the monooxygenase EthA, respectively. The activated forms react with NAD^+ to form an INH-NAD or ETH-NAD adduct. The enzymes

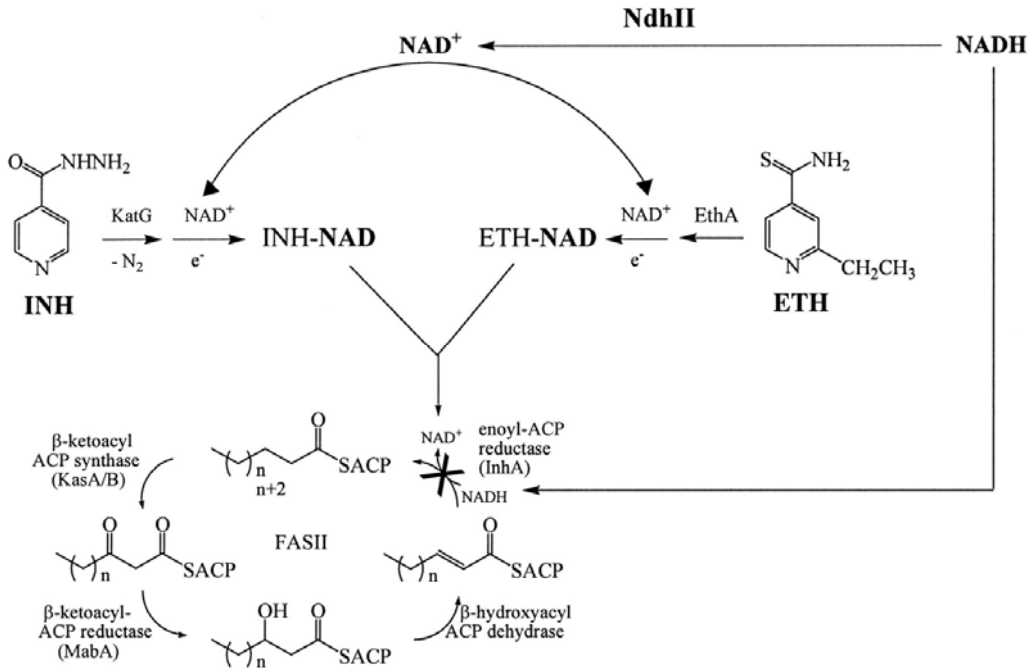

InhA and NADH-dependent enoyl-ACP reductase of the fatty acid synthase type II system are inhibited by these two adducts which leads to the inhibition of mycolic acid biosynthesis and cell lysis.The stimulators of INH and ETH drugs are katG and ethA respectively. Recessive mutations in the katG and ethA genes create resistance to INH or ETH by stopping the activation of the drugs. Creating dominant mutation in the common target enzyme InhA, can induce co-resistance to INH and ETH drugs. This mutation will lead to a change in the target enzyme integrity. The Ndh enzyme is involved in increasing the intracellular concentration of NADH. Recessive mutations in Ndh gene will cause drug resistance by inhibiting competitively the association of INH-NAD or ETH-NAD adduct with InhA. This is a novel mechanism of co-resistance to INH and ETH (15).

In the current methods of treatment, the pro-drug isoniazid (INH) was found to destroy the bacterial cell wall by inhibiting the mycolic acid synthesis which is the significant constituent of integrated cell wall. (16). INH stimulated by KatG, a catalase-peroxidase enzyme inhibits InhA, the FabI enoyl reductase (ENR) in the fatty acid synthesis (FAS-II) pathway. The activated form of INH later reacts with NAD^+ to form INH-NAD adduct (17–21). Mutations in KatG, in significant number of the strains make them resistant to INH (22–25). Therefore, the discovery of an InhA inhibitor which can avoid this initial activation step should be effective against INH resistant strains of Mycobacterium tuberculosis (MTB).

3. MATERIALS AND METHODS:

3.1. Dataset and molecular modeling

A dataset of 28 Arylamide analogues reported to have Enoyl acyl carrier protein reductase inhibitory activities (26) were used for the following QSAR studies (Table 1). In vitro inhibitory concentrations (IC50) of the molecules against Enoyl acyl carrier protein reductase were converted into corresponding pIC50 values and used as dependent variables in the 3D-QSAR calculations.

All the molecules were divided into two training sets (20 compounds) for generating 3D-QSAR models and a test set (8 compounds respectively) for validating the quality of the models. The test set was selected based on the criteria given by Oprea et al (27).

All molecular studies were performed using the molecular modeling package SYBYL 6.7.1 (28) on silicon graphics work-station. Energy

minimization was performed in SYBYL using Tripos force field (29). The conformations were generated for the most active compounds 41. As the compound is relatively rigid we have used systematic search method with a step size of 158 torsion angle to generate the conformational model. The lowest energy conformer was selected and further geometry optimization of each molecule was carried out with MOPAC 6 package using the semi-empirical AM1 Hamiltonian (20). Optimized structures with MOPAC charges were used for subsequent calculations. This conformer was considered for the building of other molecules.

3.2. Alignment

In the standard CoMSIA procedure, bioactive conformations are desired for superimposing ligand. In the absence of available crystallographic data information on Enoyl acyl carrier protein reductase and inhibitor complexes, we assumed that the active conformer corresponds to the lowest energy conformer of the conformational model. The molecular alignment was done with the atom-based RMS fit method using the command ALIGN DATABASE present in SYBYL. This option aligns the structures by pair-wise atom super positioning and all structures in the database are arranged with the same frame of reference as the template compound. The most active compound 24 was used as template and the remaining molecules were aligned to it through using the basic core of Arylamide respectively. The aligned molecules are shown in Fig. 1.

3.3. CoMSIA interaction energy fields

The CoMSIA method is based on molecular similarity indices. Using a common probe atom, similarity indices were calculated for a data set of prealigned molecules at regularly spaced grid points. There is sudden rise in energy when the atoms of the molecules approach the probe atom. Therefore, the cut off value of >30 kcal/mol is included in CoMFA. This restriction may give some false interaction energy field values, which sometimes lead to error in the predictions. The Gaussian type distance dependent functional forms used by CoMSIA method to calculate such properties overcome this problem. Similarity indices were calculated at all grid points inside and outside the molecules and evaluated in a PLS analysis following the usual CoMFA protocol.

3.4. PLS analysis

The regression analysis of CoMSIA field energies was performed using the partial least squares (PLS) algorithm with the leave-one-out (LOO) method adopted for cross validation. The optimum number of components to be used in conventional analyses was chosen from (i) the analysis with the highest cross validated r2 value, and (ii) the model with the smallest standard error of prediction for component models with identical r2 values. The column filtering value was set to 2.0 for cross validated runs. Equal weightage was assigned to steric and electrostatic fields. Final analysis was carried out to calculate the conventional r2 value using the optimum number of components.

4. RESULTS AND DISCUSSION

The predictive 3D-QSAR models were generated for the training sets of Enoyl acyl carrier protein reductase inhibitors using default parameters of COMSIA, as determined by cross validation. Reliability of the QSAR models was statistically validated using several statistical parameters, such as r2, q2 and r2 pred. A total of 28 compounds were partitioned into a training set of 20 and a test set of 8 compounds at random. Bias was given to both structural and biological diversity in both the sets. Table 3 and 4 lists the experimental activities, predicted activities and residual values of the training set and test set by CoMSIA model. The CoMSIA models yielded a good cross-validated correlation coefficient with LOO of 0.744 and with leave-many-out (q2 with 10 groups) was 0.743, thus the predictions obtained with these models were reliable. These internal validation methods (leave-one-out and leave-one-out) determine the stability of the developed models.

The non-cross-validated PLS analysis evaluated the correlation coefficient value $(r)^2$ as 0.901 and the standard error of estimate (SEE) was observed as 0.118.

Table 1 : 28 molecules Structures and activities of the molecules

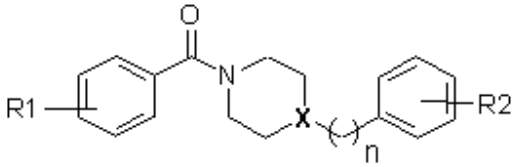

Compound	X	n	R1	R2	IC50 [uM]	pIC50
1	N	0	H	H	38.86	4.410
2	N	0	4-CH3	H	16.64	4.779
3	N	0	4-CH3	3-CF3	6.26	5.203
4	N	0	4-CH3	3-Cl	3.07	5.513
5	N	0	3-CH3	3-Cl	9.43	5.025
6	N	0	3-CH3	4-NO2	15.47	4.811
7	N	0	3,4-Me2	3-Cl	0.99	6.004
8	N	0	3,4-Me2	3-CF3	1.85	5.733
9	N	0	4-i-Pr	3-Cl	100	4.000
10	N	0	4-t-Bu	3-Cl	100	4.000
11	N	0	4-t-Bu	3-CF3	100	4.000
12	N	0	4-t-Bu	4-CH3,	100	4.000
13	N	0	2-F	3-Cl	13.87	4.858
14	N	0	4-F	3-Cl	9.74	5.011
15	N	0	3-Cl	3-Cl	6.73	5.172
16	N	0	3,4-Cl2	3-Cl	6.05	5.218
17	N	0	3,4-Cl2	H	17.62	4.754
18	N	1	H	H	31.5	4.502
19	C	1	3-Cl	H	7.74	5.111
20	C	1	2-F	H	14.11	4.850
21	C	1	4-CH3	H	5.16	5.287
22	C	1	3-CH3	H	7.39	5.131
23	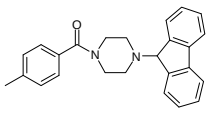				0.40	6.398
24	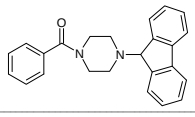				0.09	7.046
25	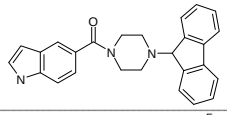				0.20	6.699
26	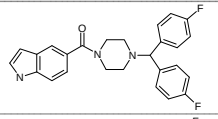				1.04	5.983
27	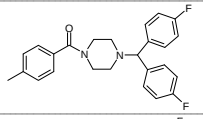				1.89	5.724
28	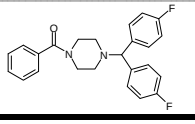				2.04	5.690

Table 2- CoMSIA PLS Result Summary

q2	*r2*	*r2pred*	*LOO*	*LMO*	*n*	*F value*	*SEE*	*Steric*	*Electrostatic*
0.901	0.987	0.900	0.744	0.743	6	169.920	0.118	0.484	0.516

Table 3: Activities and residuals of training set for CoMSIA models

Compound	pIC50	CoMSIA	
		Predicted	Residual
10	4	4.076	-0.076
11	4	4.057	-0.057
12	4	3.884	0.116
13	4.857	5.19	-0.333
14	5.011	4.997	0.014
15	5.171	4.817	0.354
17	4.753	5.003	-0.25
2	4.778	4.65	0.128
5	5.025	4.8	0.225
6	4.81	4.968	-0.158
8	5.732	5.458	0.274
9	4	4.388	-0.388
20	4.85	5.353	-0.503
21	5.287	5.041	0.246
22	5.131	5.452	-0.321
23	6.397	6.34	0.057
24	7.045	6.7	0.345
25	6.698	6.558	0.14
27	5.723	5.236	0.487
28	5.69	5.684	0.006

Table 4: Activities and residuals of test set for CoMSIA models

Compound	PIC50	CoMSIA	
		Predicted	Residual
1	4.41	4.927	-0.617
16	5.218	4.859	0.359
3	5.203	5.58	0.523
4	5.512	5.656	0.856
7	6.004	5.511	0.493
18	4.502	4.351	
19	5.111	5.695	-0.584
22	5.131	5.53	-0.399

Fig 1: Alignment of 28 molecules

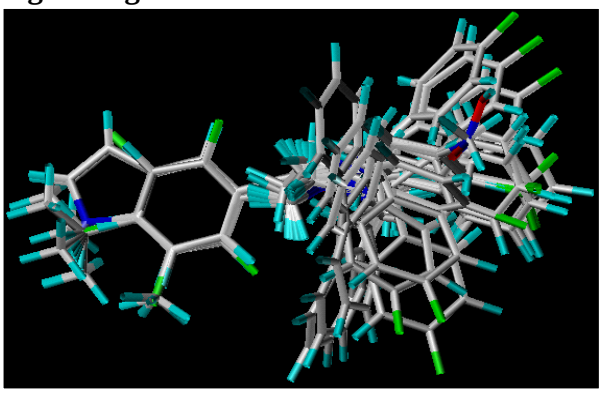

Contour Maps

1) **Electrostatic contour maps of least active compound 10**

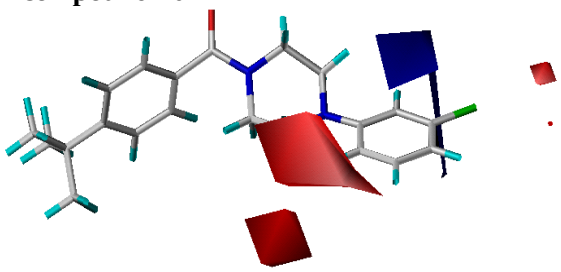

2) **Steric contour maps of least active compound 10**

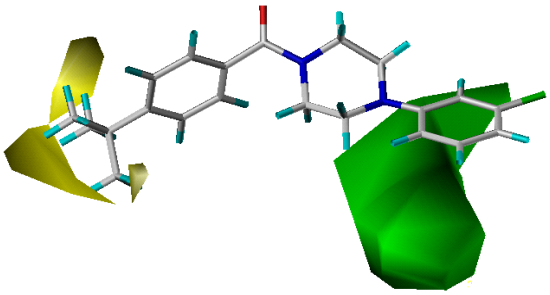

3) **Electrostatic contour maps of most active compound 24**

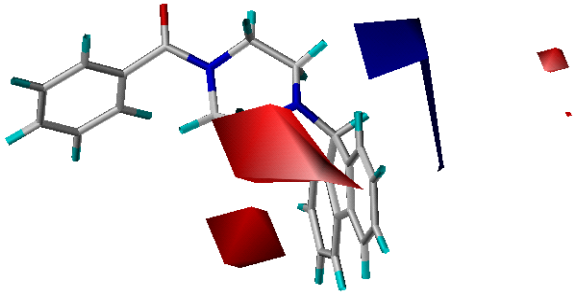

4) Steric contour maps of most active compound 24

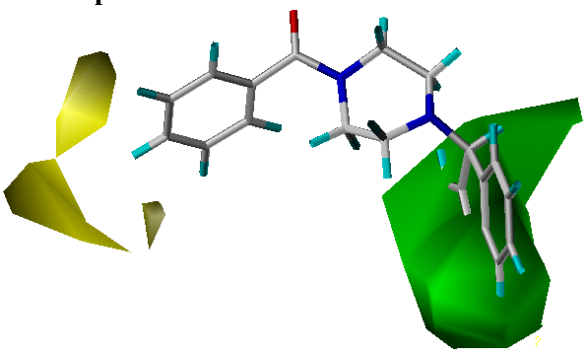

F-value stands for the degree of statistical confidence on the developed models and the model has good value of 169.920. The statistical data obtained from the standard CoMSIA model constructed with steric and electrostatic fields are depicted in Table 2. The steric and electrostatic contributions are 48.4% and 51.6%, respectively.

5. CONCLUSION

In the current study, we have successfully established the ligand–based 3D QSAR CoMSIA model on 28 Arylamide derivatives, reported as enoyl acyl carrier protein reductase inhibitors. This model has good statistical results in terms of q2 and r2 values and showed a great predictivity of the test set, in the external validation, without visible outliers. The model gave q2 and r2 values of 0.901 and 0.987. The CoMSIA results suggest that steric interactions (48.4%) as well as electrostatic interactions (51.6%) contribute to the activities of inhibitors. The effect of steric and electrostatic fields around aligned molecules was clarified by analyzing CoMSIA contour maps. This comparative analysis of contour maps is expected to be of an aid in the design of compounds with an enhanced inhibitory activity and better selectivity to enoyl acyl carrier protein reductase.

6. REFERENCES

[1]. WHO Report, 2007, <www.who.int/tb/publications/ global_ report / 2007/pdf/full.pdf>.

[2]. Aziz, M. A.; Wright, A.; Laszlo, A.; De Muynck, A.; Portaels, F.; Van Deun, A.; Wells, C.; Nunn, P.; Blanc, L. Epidemiology of antituberculosis drug resistance (the Global Project on Anti-tuberculosis Drug Resistance Surveillance): an updated analysis M. *Lancet 2006; 368: 2142-54*

[3]. Raviglione, M. C.; Smith, I. M. N. Engl. XDR Tuberculosis — Implications for Global Public Health *J. Med. 2007; 356: 656-659*

[4]. Pasqualoto, K. F.; Ferreira, E. I.; Santos-Filho, O. A.; Hopfinger, A. J. *Rational design of new antituberculosis agents: receptor-independent four-dimensional quantitative structure-activity relationship analysis of a set of isoniazid derivatives J Med Chem. 2004 Jul 15;47(15):3755-64.*

[5]. Wei, C. J.; Lei, B.; Musser, J. M.; Tu, S. C. Isoniazid Activation Defects in Recombinant Mycobacterium tuberculosis Catalase-Peroxidase (KatG) Mutants Evident in InhA Inhibitor Production *Antimicrob. Agents Chemother. 2003; 47: 670-675*

[6]. Morlock, G. P.; Metchock, B.; Sikes, D.; Crawford, J. T.; Cooksey, R. C. ethA, inhA, and katG Loci of Ethionamide-Resistant Clinical Mycobacterium tuberculosis Isolates *Antimicrob. Agents Chemother. 2003; 47: 3799-3805.*

[7]. Ormerod, L. P. Multidrug-resistant tuberculosis (MDR-TB): epidemiology, prevention and treatment Br Med Bull 2005; 73-74: 17-24.

[8]. Zhao, X.; Yu, S.; Magliozzo, R. S. Characterization of the binding of isoniazid and analogues to Mycobacterium tuberculosis catalase-peroxidase *Biochemistry 2007; 46: 3161-70.*

[9]. Rawat, R.; Whitty, A.; Tonge, P. J. The isoniazid-NAD adduct is a slow, tight-binding inhibitor of InhA, the Mycobacterium tuberculosis enoyl reductase: adduct affinity and drug resistance Proc. Natl. Acad. Sci. USA 2003; 100(24), 13881-6.

[10]. Schaeffer, M. L.; Agnihotri, G.; Volker, C.; Kallender, H.; Brennan, P. J.; Lonsdale, J. T. Purification and biochemical characterization of the Mycobacterium tuberculosis beta-ketoacyl-acyl carrier protein synthases KasA and KasB *J. Biol. Chem. 2001; 276: 47029-37.*

[11]. Kuo, M. R.; Morbidoni, H. R.; Alland, D.; Sneddon, S. F.; Gourlie, B. B.; Staveski, M. M.; Leonard, M.; Gregory, J. S.; Janjigian, A. D.; Yee, C.; Kreiswirth, B.; Iwamoto, H.; Perozzo, R.; Jacobs, W. R., Jr.; Sacchettini, J. C.; Fidock, D. A. Targeting Tuberculosis and Malaria Through Inhibition of Enoyl Reductase: Compound Activity and Structural Data *J. Biol. Chem. 2003; 278: 20851-59.*

[12]. Choi, K. H.; Kremer, L.; Besra, G. S.; Rock, C. O. Identification and substrate specificity of beta - ketoacyl (acyl carrier protein) synthase III

(mtFabH) from Mycobacterium tuberculosis *J. Biol. Chem. 2000; 275: 28201-7.*

[13]. Kremer, L.; Douglas, J. D.; Baulard, A. R.; Guy, M. R.; Morehouse, C.; Alland, D.; Dover, L. G.; Lakey, J. H.; Jacobs, W. R., Jr.; Brennan, P. J.; Minnikin, D. E.; Besra, G. S. Thiolactomycin and Related Analogues as Novel Anti-mycobacterial Agents Targeting KasA and KasB Condensing Enzymes in Mycobacterium tuberculosis J. *Biol. Chem. 2000; 275: 16857-64.*

[14]. Ducasse-Cabanot, S.; Cohen-Gonsaud, M.; Marrakchi, H.; Nguyen, M.; Zerbib, D.; Bernadou, J.; Daffe, M.; Labesse, G.; Quemard, A. In Vitro Inhibition of the Mycobacterium tuberculosis ß-Ketoacyl-Acyl Carrier Protein Reductase MabA by Isoniazid *Antimicrob. Agents Chemother.2004; 48: 242-249.*

[15]. Altered NADH/NAD+ Ratio Mediates Coresistance to Isoniazid and Ethionamide in Mycobacteria *Antimicrob. Agents Chemother. 2005; 49: 708-720.*

[16]. Brennan, P. J.; Rooney, S. A.; Winder, F. G. Ir. The lipids of Mycobacterium tuberculosis BCG: fractionation, composition, turnover and the effects of isoniazid *J. Med. Sci. 1970; 3: 371-390.*

[17]. Johnsson, K.; King, D. S.; Schultz, P. G. Studies on the mechanism of action of isoniazid and ethionamide in the chemotherapy of tuberculosis J. Am. Chem.Soc. 1995; 117: 5009-5010.

[18]. Marcinkeviciene, J. A.; Magliozzo, R. S.; Blanchard, J. S. Purification and Characterization of the Mycobacterium smegmatis Catalase-Peroxidase Involved in Isoniazid Activation *J. Biol. Chem. 1995; 270: 22290-22295.*

[19]. Basso, L. A.; Zheng, R. J.; Blanchard, J. S. Kinetics of inactivation of WT and C243S mutant of Mycobacterium tuberculosis enoyl reductase by activated isoniazid. J. Am. Chem.Soc. 1996; 118: 11301-2.

[20]. Quemard, A.; Dessen, A.; Sugantino, M.; Jacobs, W. R., Jr.; Sacchettini, J. C.; Blanchard, J. S. Binding of Catalase-Peroxidase-Activated Isoniazid to Wild-Type and Mutant Mycobacterium tuberculosis Enoyl-ACP Reductases *J. Am. Chem. Soc. 1996; 118: 1561-1562.*

[21]. Rawat, R.; Whitty, A.; Tonge, P. J. The isoniazid-NAD adduct is a slow, tight-binding inhibitor of InhA, the Mycobacterium tuberculosis enoyl reductase: adduct affinity and drug resistance Proc. Natl. Acad. Sci.U.S.A. 2003; 100: 13881-13886.

[22]. Zhang, Y.; Heym, B.; Allen, B.; Young, D.; Cole, S. The catalase-peroxidase gene and isoniazid resistance of Mycobacterium tuberculosis *Nature 1992; 358: 591-593.*

[23]. Stoeckle, M. Y.; Guan, L.; Riegler, N.; Weitzman, I.; Kreiswirth, B.; Kornblum, J.; Laraque, F.; Riley, L. W. Catalase-peroxidase gene sequences in isoniazid-sensitive and -resistant strains of Mycobacterium tuberculosis from New York City *J. Infect. Dis. 1993; 168: 1063-5.*

[24]. Musser, J. M.; Kapur, V.; Williams, D. L.; Kreiswirth, B. N.; van Soolingen, D.; van Embden, J. D. *Characterization of the catalase-peroxidase gene (katG) and inhA locus in isoniazid-resistant and -susceptible strains of Mycobacterium tuberculosis by automated DNA sequencing: restricted array of mutations associated with drug resistance J. Infect. Dis. 1996; 173: 196-202.*

[25]. Ramaswamy, S. V.; Reich, R.; Dou, S. J.; Jasperse, L.; Pan, X.; Wanger, A.; Quitugua, T.; Graviss, E. A. Single Nucleotide Polymorphisms in Genes Associated with Isoniazid Resistance in Mycobacterium tuberculosis *Antimicrob. Agents Chemother. 2003; 47: 1241-1250.*

[26]. Xin He, Akram Alian and Paul R. Ortiz de Montellano, Inhibition of the Mycobacterium tuberculosis enoyl acyl carrier protein reductase InhA by arylamides, Bioorganic & Medicinal Chemistry 15 [2007] 6649-6658

[27]. T.I. Oprea; C.L. Waller; G.R. Marshall. Three-dimensional quantitative structure-activity relationship of human immunodeficiency virus (I) protease inhibitors. 2. Predictive power using limited exploration of alternate binding modes. *J. Med. Chem. 37 [1994] 2206-2215.*

[28]. Sybyl 6.7.1, Tripos Inc., 1699 South Hanely Road, St. Louis, Missouri, 63144, USA.

[29]. M. Clark; R.D. Cramer III; N.V. Opdenbosch. Validation of the general purpose Tripos 5.2 forcefield. *J. Comput. Chem. 10 [1989] 982-1012.*

[30]. M.J.S. Dewar; E.G. Zoebisch; E.F. Healy; J.J.P. Stewart. Development and use of quantum mechanical molecular models. 76. AM1: a new general purpose quantum mechanical molecular model. *J. Am. Chem. Soc. 107 [1985] 3902-3909.*